SOILS AND FOUNDATIONS Vol. 37, No. 3, 79-94, Sept. 1997
Japanese Geotechnical Society

PRELOADED AND PRESTRESSED REINFORCED SOIL

FUMIO TATSUOKA[i], TARO UCHIMURA[ii] and MASARU TATEYAMA[iii]

ABSTRACT

A new construction method is described which aims at making reinforced soil structures, such as a geosynthetic-reinforced soil bridge abutment, very stiff and elastic. To make the deformation of a reinforced soil mass nearly elastic, a large preload is first applied by introducing tension into metallic tie rods which penetrate the reinforced soil and are connected to top and bottom reaction blocks. The tensile force in the tie rods functions as a prestress increasing the confining pressure and the stiffness of the soil is kept high. Compressive or tensile surcharge loads applied to the top block are supported by both the tie rods in tension and the soil mass in compression. Prestress is introduced in the reinforcement by preloading the tie rods, which contributes to maintaining the integrity of the soil mass. A working example and the result of a full-scale test are presented.

Key words: creep, preload, prestress, reinforced soil, relaxation (**IGC**: E2/H2)

INTRODUCTION

One of the inherent drawbacks of uncemented soils (i.e., most types of clays, sands and gravels) is their low stiffness under low confining pressure and zero stiffness when subjected to tensile load. For this reason, a soil mass may exhibit intolerable compression when subjected to large compressive load, while it shows no resistance against tension. Even when a soil mass is reinforced with horizontal tensile reinforcement members (e.g., steel strips or planar geosynthetic sheets), the soil mass may not become much stiffer under vertical surcharge load than an unreinforced soil. This point can be seen, for example, from the model test results shown in Fig. 1: the initial coefficient of vertical subgrade reaction (i.e., initial stiffness), which is the ratio of the footing load to the footing settlement at the initial loading stage, is not significantly larger when reinforced soil is used. The ultimate footing load, however, increases extensively with reinforcing.

A similar problem with reinforced concrete (RC) beams and piles can be effectively overcome by introducing pre-tension and pre-compression to steel reinforcement and concrete, respectively (Fig. 2). When a tensile load P_T is applied to the element A with cracks in the concrete that have appeared in the direction orthogonal to the loading direction, P_T is supported only by the steel reinforcement. When the tensile rigidity of the steel reinforcement is K_{rod}, the elongation is obtained as;

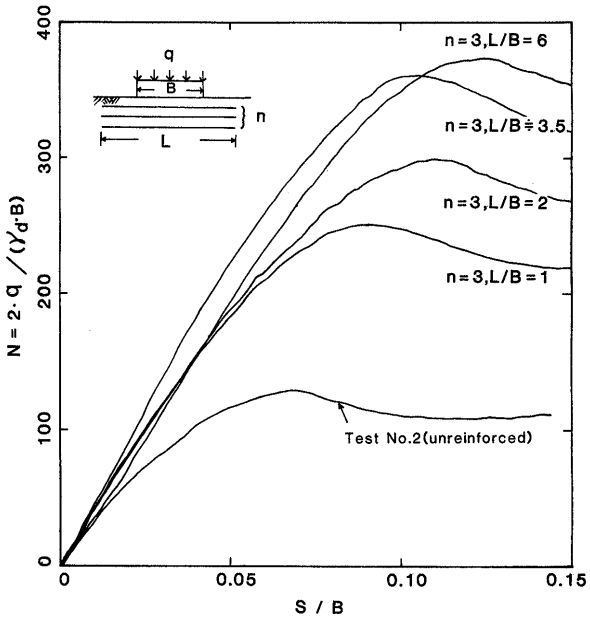

Fig. 1. Relationships between the normalized footing pressure $N=2q/(\gamma \cdot B)$ and the settlement ratio S/B from plane strain model tests of a strip footing on unreinforced and reinforced dense Toyoura sand (D_r=80-86%); q is the average footing pressure, B is the footing width (10 cm), γ_d is the sand unit weight (1.58 gf/cm^3 or 1.55 kN/m^3); the reinforcement is twenty four phosphor bronze strips for a 40 cm (sand box width), each having a width of 0.3 cm, a thickness of 0.3 cm and the Young's modulus=1.24×10^5 kgf/cm^2 (1.22×10^7 kN/m^2) (Fig. 7 of Huang and Tatsuoka, 1990)

[i] Professor, Dept. of Civil Engineering, University of Tokyo, 7-3-1, Hongo, Bunkyo-ku, Tokyo 113.
[ii] Research Assistant, ditto.
[iii] Research Engineer, Railway Technical Research Institute.
Manuscript was received for review on January 12, 1996.
Written discussions on this paper should be submitted before April 1, 1998 to the Japanese Geotechnical Society, Sugayama Bldg., 4F, Kanda Awaji-cho, 2-23, Chiyoda-ku, Tokyo 101, Japan. Upon request the closing date may be extended one month.

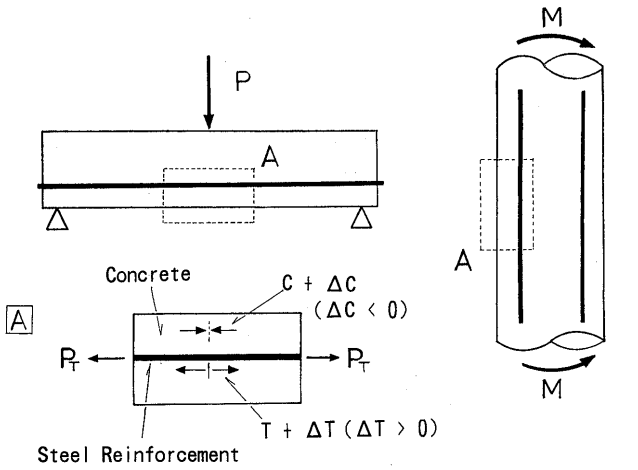

Fig. 2. Schematic diagram of prestressed RC beam and pile

$$S_1=P_T/K_{rod} \tag{1}$$

When the pre-tension T (positive in tension) has been introduced into the reinforcement with the corresponding pre-compression C (positive in compression) in the concrete mass, the load equilibrium when the tensile force P_T is applied to the element A is;

$$P_T=\Delta T-\Delta C=\Delta T+(-\Delta C) \tag{2}$$

where ΔT is the increase in the tensile force T and $(-\Delta C)$ is the decrease in the compressive force C due to the application of P_T (i.e., ΔC is negative in this case). The elongation S_2 is the same for the reinforcement and the concrete mass, which is given by;

$$S_2=\Delta T/K_{rod}=(-\Delta C)/K_{concrete} \tag{3}$$

where $K_{concrete}$ is the rigidity of the concrete mass of the element A in compression. It should be noted that non-uniform stress and strain distributions for each of the concrete mass and reinforcement are ignored in this simplified discussion. From Eqs. (2) and (3), we obtain;

$$S_2=P_T/(K_{rod}+K_{concrete}) \tag{4}$$

Equation (4) indicates that as far as the stress in the concrete is compressive or the concrete exhibits resistance against tension as against compression, the total stiffness K is $K_{rod}+K_{concrete}$, which is larger than K_{rod}, the value when the concrete does not resist tension.

A new construction method is proposed herein which applies the principle of prestressed (PS) reinforced concrete to a reinforced soil mass subjected not only to tensile load but also to compressive load (Fig. 3(a)). In the case illustrated in Fig. 3(a), the top and bottom ends of tie rods are anchored to the top and bottom reaction blocks, which confine a soil mass reinforced with tensile reinforcement layers placed horizontal. This type of reinforced soil will herein be called "the preloaded/prestressed (PL/PS) reinforced soil". Consideration of some important inherent soil characteristics, including visco-elasto-plastic deformation characteristics and the dependency of the stiffness on pressure level, makes this method unique.

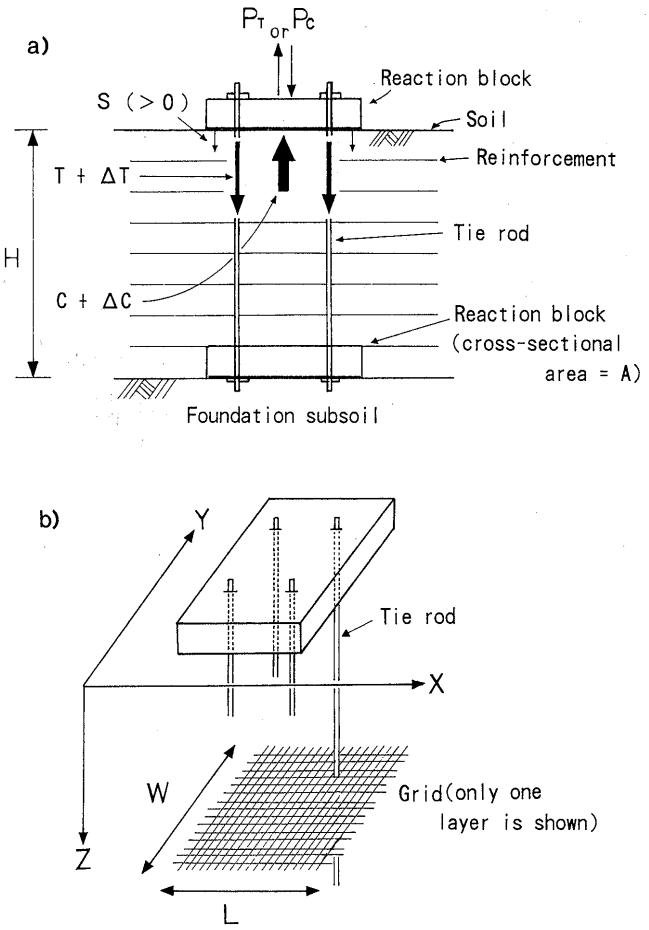

Fig. 3. a) Schematic diagram of a reinforced soil mass subjected to external tensile and compressive load, b) Three-dimensional configuration

PRESTRESSING SOIL

When tensile prestress is introduced into the tie rods penetrating a reinforced soil mass as shown in Fig. 3(a), similar to the case of PS reinforced concrete, the soil mass can resist some tensile load P_T applied to the top block to which the tie rods are anchored. In this case, the working principle is the same as that for PS reinforced concrete;

$$P_T=\Delta T+(-\Delta C) \tag{2 bis}$$

where ΔT is the increase in the total tensile force T in the tie rods and $(-\Delta C)$ is the decrease in the compressive force C in the soil mass from the application of P_T. The elongation S_2 is the same for the tie rods and the soil mass, which is given by;

$$S_2=\Delta T/K_{rod}=(-\Delta C)/K_{soil} \tag{5}$$

where K_{soil} is the rigidity of the soil mass in compression (i.e., K_{soil} is the coefficient of vertical subgrade reaction times the cross-sectional area A of the reaction block). From Eqs. (2 bis) and (5), we obtain;

$$S_2=P_T/(K_{rod}+K_{soil}) \quad (6)$$

As far as the vertical stress at the top surface of the soil mass is in compression, the rigidity of the soil-rod-block system is given by Eq. (6), which is larger than K_{rod} for the case where no pre-compressive force is applied at the top of the soil mass.

Advantages of prestressing can also be expected when the vertical load is in compression, P_C. That is, referring to Fig. 3(a), we obtain;

$$P_C=(-\Delta T)+\Delta C \quad (7)$$

where $(-\Delta T)$ is the decrease in the total tensile force T in the tie rods and ΔC is the increase in the compressive force C in the soil mass from the application of P_C (n.b., ΔT is negative in this case). The compression S_2 is the same for the tie rods and the soil mass, given by;

$$S_2=(-\Delta T)/K_{rod}=\Delta C/K_{soil} \quad (8)$$

From Eqs. (7) and (8), we obtain;

$$S_2=P_C/(K_{rod}+K_{soil}) \quad (9)$$

As far as the axial stress in the tie rods is in tension, Eq. (9) is valid and the rigidity of the soil-rod-block system is larger than K_{soil}. It is reasonable to assume that measurable large stiffness of the tie rods cannot be expected when the axial stress in the tie rods is in compression. It is apparent that for both cases of tensile and compressive loads, P_T and P_C, the deformation S_2 of the backfill soil and tie rods decreases with the increase in the soil stiffness K_{soil}. Different from concrete, soil exhibits larger stiffness as the confining pressure increases.

Lateral strains due to vertical load in a soil mass reinforced with stiff lateral reinforcement would be much smaller than vertical strains. The value of K_{soil} can then be related to the one-dimensional compressibility m_v, which is equal to the inverse of the constraint modulus M, without a large error, as;

$$K_{soil}=A/(m_v\cdot H) \quad (10)$$

where A is the base area of the reaction block, which is assumed to be equal to the horizontal cross-sectional area of the reinforced soil mass and effectively resists the applied load P_T or P_C; H is the height of the reinforced soil mass; and M is the average one-dimensional compressibility for the soil mass. For an isotropic soil mass, m_v is obtained as;

$$m_v=\{(1+\nu)(1-2\nu)/(1-\nu)\}/E \quad (11)$$

where E and ν are the average drained Young's modulus and drained Poisson's ratio for the soil mass. For a small strain range of less than about 0.05 %, which is the main concern in this study, the ν value for gravel is around 0.2 (Dong et al., 1994). $M=1/m_v$ becomes then very close to E, and Eq. (10) can be approximated by;

$$K_{soil}=A\cdot E/H \quad (12)$$

In case tensile lateral strains take place to some extent when vertical load is applied to the reinforced soil mass, Eq. (12) becomes more appropriate. In a more rigorous analysis described later, the soil stiffness is defined as the tangent stiffness which is a function of the overburden pressure considering the surcharge load and the weight of the soil.

Since the soil stiffness increases with an increase in confining pressure, a larger tensile force T in the tie rods results in larger soil stiffness. However, the introduction of large tension in the tie rods, i.e., large compression in the soil mass, may lead to the failure of the soil mass if it is not effectively reinforced. Reinforcing soil with the use of sufficiently stiff and strong tensile reinforcement members is, therefore, essential for introducing a tensile load which is large enough to make the proposed method effective in stiffening a soil mass. It should be noted that when the reinforced soil mass to be preloaded has finite dimensions (width and length) as shown in Fig. 3(b), the soil mass should be effectively reinforced in both directions (i.e., in the x and y directions). For this purpose, the use of reinforcement having similar stiffness in the orthogonal directions, such as a bi-axial grid, is appropriate. When metal strips are used, however, they should be placed in both orthogonal directions.

For ground anchors, anchor tendons are prestressed to increase the confining pressure in the subsoil in order increase the shear strength and rigidity of the soil. Many aspects of this established technology are utilized for the proposed construction method. There have been several cases where prestress was introduced in vertical anchor tendons installed in the existing subsoil so as to increase the vertical rigidity of an anchor-soil system supporting a slender structure subjected to dynamic loading (e.g., Luong, 1990, 1991).

PRELOADING SOIL

Different from concrete, soil may exhibit the noticeable property of viscous deformation. For this reason, prestress may relax very rapidly after the top ends of the tie rods are fixed to the top block. In that case, the advantages of prestressing described above will rapidly decrease.

The rate of creep deformation and stress relaxation should decrease substantially by applying sufficiently large preload during construction and allowing sufficiently large creep deformation of the soil to occur during preloading. This behaviour can be expected if the visco-elasto-plastic property of the soil can be modeled by the three component 1-D rheology model shown in Fig. 4(a) (Di Benedetto, 1983). That is, the component EP1 exhibits one type of time-independent elasto-plastic property, while the component EP2 exhibits another type of time-independent elasto-plastic property and the dashpot DP exhibits viscous property. The strain ε of the whole system is the sum of the strain ε_1 occurring in EP1 and the strain ε_2 occurring in EP2 and DP. The stress σ at EP1, which is the stress applied to the whole system, is equal to the sum of the stress σ_2 at EP2 and the stress σ_{DP} at DP. In this model, the rate of creep deformation and

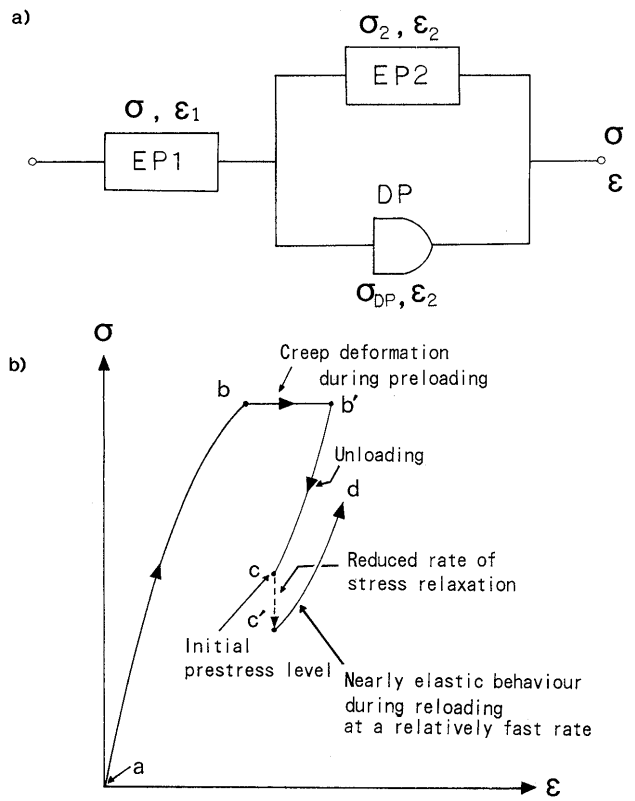

Fig. 4. a) Three-component rheology model proposed by Di Benedetto (1983) (Di Benedetto and Tatsuoka, 1996), b) Schematic diagram showing the effect of preloading on the property after unloading

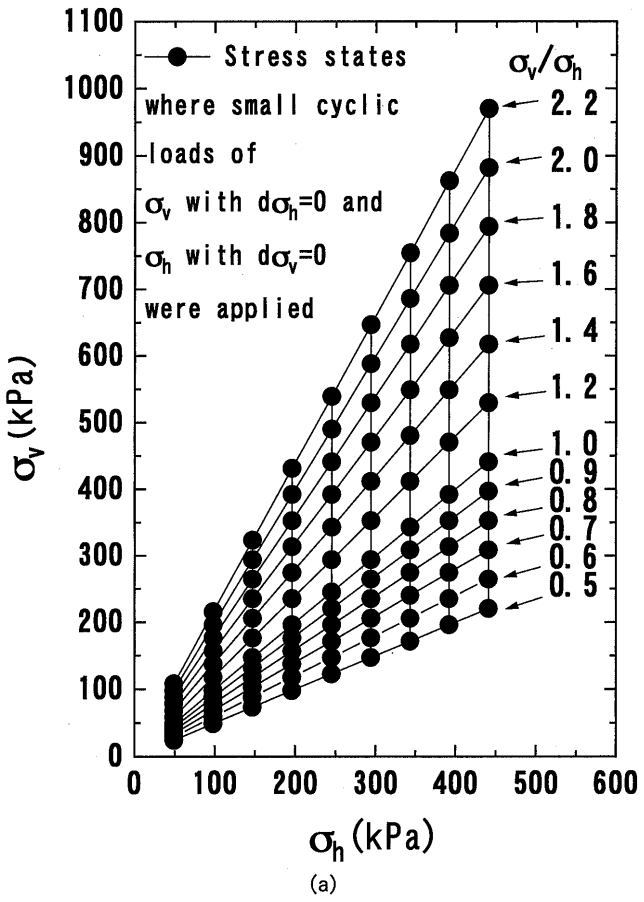

Fig. 5. a) Stress states where elastic deformation characteristics were evaluated, b) E_v as a function of σ_v; a densely compacted well-graded gravel of crushed sandstone (Jiang, 1996)

stress relaxation at a given stress level decreases as EP2 and DP are increasingly strained; i.e., as the stress σ_2 at EP2 increases and the stress σ_{DP} at DP decreases. This situation can be attained by allowing larger creep deformation to occur at a stress level that is higher than the current stress level (Fig. 4(b)).

Another important positive effect of preloading on the soil stiffness is to substantially reduce plastic deformation for a given relatively small stress increment during reloading (e.g., from c′ to d in Fig. 4(b)). It is known that for granular materials, the tangent Young's modulus $E_i=d\sigma_i/d\varepsilon_i$ defined for the major principal elastic strain increment $d\varepsilon_i$ in a certain direction, which is positive in compression, is a rather unique function of the normal stress σ_i working in that direction (Kohata et al., 1994; Tatsuoka and Kohata, 1995; Hoque et al., 1995). A typical result for gravel is shown in Fig. 5. A rectangular prism specimen (57 cm high and 23 cm × 23 cm in cross-section) of very dense well-graded gravel consisting of crushed sandstone having $D_{max}=37.5$ mm, $D_{50}=4$ mm, $U_c=6.4\,\text{mm}/0.09\,\text{mm}=71$ and a fines content equal to 8.0% was prepared at a water content equal to 6.8% by using a small vibrator placed on the surface of each of fourteen sub-layers of the specimen (Jiang, 1996). The initial dry density was 1.80 gf/m^3 and the initial void ratio was 0.49. At different stress states under triaxial stress conditions (Fig. 5(a)), the vertical elastic Young's modulus E_v defined for a single axial strain amplitude of the order of 0.001% was evaluated by applying very small cyclic axial stresses σ_v at a constant lateral stress σ_h. The horizontal value E_h was obtained by applying very small cyclic lateral stresses σ_h with a constant σ_v. In order to eliminate the effects of bedding error and membrane penetration, axial and lateral strains were measured locally by using, respectively, a pair of local deformation transducers (LDTs; Goto et al., 1991) that were set vertically and eight LDTs that were set laterally on the surface of the specimen (Hoque et al., 1995). It can be seen from

Fig. 5(b) that the Young's modulus E_v is a rather unique function of σ_v. Similarly, it has been found that E_h is a rather unique function of σ_h (Jiang, 1996). This result indicates that as the tensile force T in the tie rods increases, the elastic soil stiffness in the vertical direction increases.

Another advantage for vertical preloading is the introduction of prestress also in reinforcement members by the ratcheting mechanism. This mechanism results from a combination of the elasto-plastic property of soil and the nearly elastic property of reinforcement. This is similar to the effects of compaction of a soil layer placed above a reinforcement layer on the tensile strains in reinforcement (McGown et al., 1991). That is, for a simple model illustrated in Fig. 6(a), suppose that lateral tensile deformation occurs within a soil mass upon vertical loading. This induces tensile force T in the elastic reinforcement member (Fig. 6(b)). Upon removal of the vertical load (Fig. 6(c)), most of the lateral strain in the soil is not recovered due to its plastic deformation. As a result, residual tensile strain and hence force T_R remains in the reinforcement after the vertical load is removed and is counter-balanced with the lateral compressive stress σ_c in the soil. The prestress in the reinforcement can contribute to the integrity of the reinforced soil mass, and may decrease to some extent the rate of creep deformation and stress relaxation of the soil subjected to vertical load.

In summary, therefore, prestressing that follows a preloading procedure can increase the stiffness of a reinforced soil mass due to the following factors:

1) Compressive prestress in the soil mass helps the tie rods in tension to resist vertical tensile load applied to the top reaction block, while tensile prestress in the tie rods helps the soil in compression to resist vertical compressive load applied to the top block.

2) With compressive prestress in the soil mass, the soil stiffness is higher than the value when prestress has not been introduced.

3) Preloading can make the deformation of soil nearly elastic for a relatively small load increment. Preloading with creep deformation allowed to occur decreases the rate of creep deformation and stress relaxation after unloading.

4) Vertical preloading introduces tensile strains (i.e., prestress) in horizontal reinforcement members, which contributes to the integrity of the soil mass.

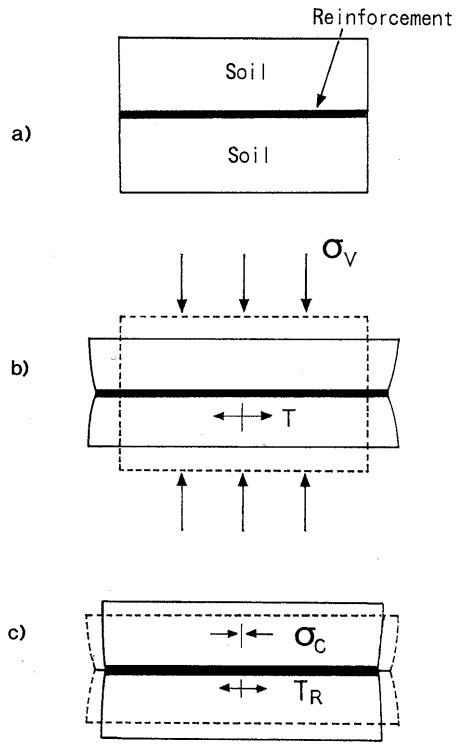

Fig. 6. Schematic diagram of ratcheting mechanism in vertical preloading of a reinforced soil mass

ESTIMATION OF DEFORMATION

The effect of preloading and prestressing was evaluated for a typical configuration of geosynthetic-reinforced gravel retaining wall. Figure 7 shows a pair of bridge abutments with backfill soil of geosynthetic-reinforced gravel constructed for the yard of the bullet train (Shinkansen) in Nagoya City. The gravel was crushed sandstone having $D_{max}=50.8$ mm, $D_{50}=4.76$ mm, $U_c=91.8$ and a fines content=9.4%. A series of triaxial compression tests were performed on cylindrical specimens (30 cm in diameter and 60 cm in height) of this material compacted to the field dry density $\gamma_d=2.21-2.25$ gf/cm^3, while axial strains were measured locally with LDTs (Dong et al., 1994; Tatsuoka et al., 1995). A typical triaxial compression test result for a specimen consolidated isotropically to a confining pressure equal to 0.2 kgf/cm^2 (19.6 kPa) is shown in Fig. 8. The axial elastic Young's modulus E_{eq} evaluated by applying very small unload/reload cycles during triaxial compression increased with the increase in the axial stress σ_a. The E_{eq} values obtained from this and other similar tests are plotted against σ_a in Fig. 9. A set of data obtained from each of the two triaxial compression tests is indicated with a broken curve. In this figure, the initial tangent Young's moduli E_0 obtained from the initial part of the primary deviator stress-axial strain relationship for a range of axial strain less than about 0.001% and the initial values of $(E_{eq})_i$ ob-

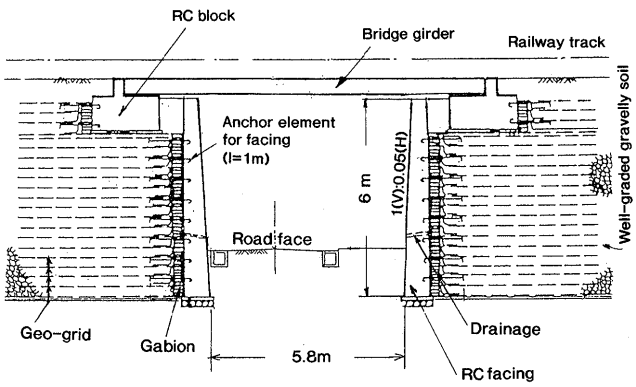

Fig. 7. A pair of geosynthetic-reinforced gravel bridge abutments for reconstructing the yard of the bullet train (Shin-kansen) in Nagoya City (Tatsuoka et al., 1992)

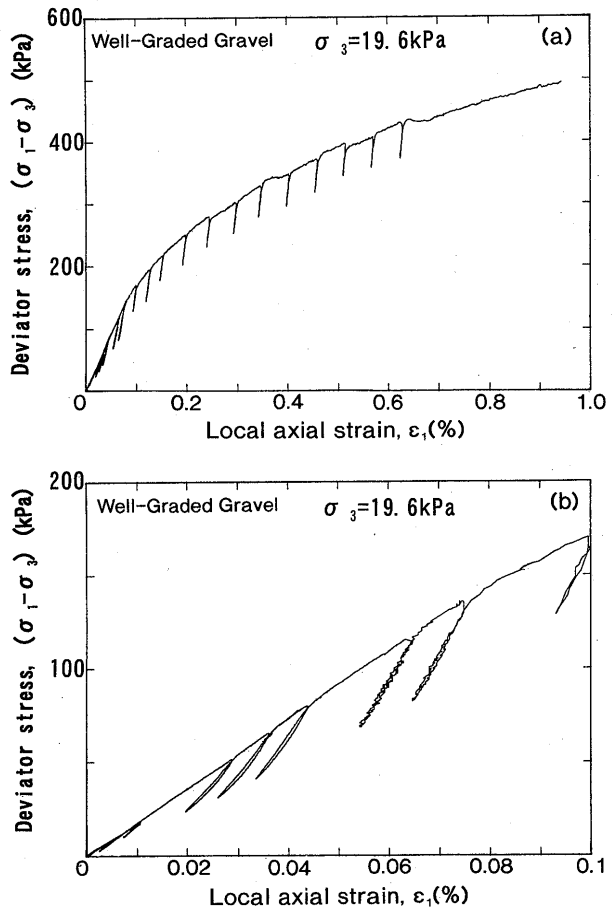

Fig. 8. Relationship between the deviator stress and the locally measured axial strain from a drained triaxial compression test (σ_3=0.2 kgf/cm^2; 19.6 kPa) on a well compacted well-graded gravel used as a backfill material of the GRS bridge abutments in Nagoya (Dong et al., 1994); a) relation up to 1% and b) 0.1%

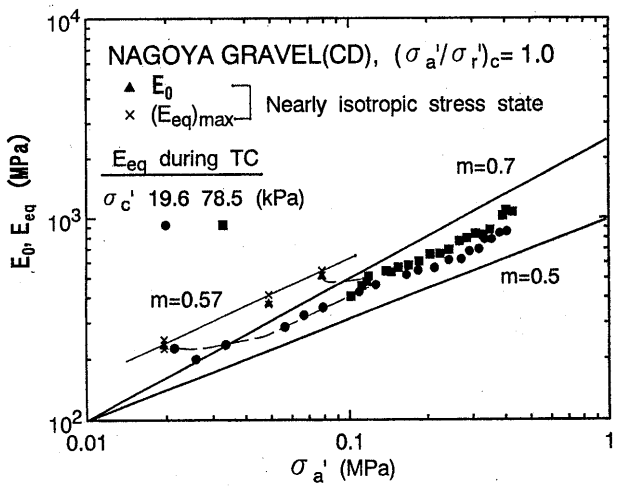

Fig. 9. Relationship between the elastic Young's moduli E_{eq} and E_{max} and the axial stress σ_a for a well compacted well-graded gravel used as a backfill material of the GRS bridge abutments in Nagoya (Dong et al., 1994)

tained from the first small unload/reload cycle applied immediately after the start of triaxial compression are also plotted. It may be seen that the elastic Young's moduli, E_{eq} and E_0, increase with the increase in σ_a not only under isotropic stress conditions but also during triaxial compression, following a similar $E_{eq}(E_0)$ and σ_a relationship. It is seen that the E_{eq} values measured at anisotropic stress states with $\sigma_a/\sigma_c=\sigma_1/\sigma_3$ larger than unity are smaller to some extent than both the E_0 and $(E_{eq})_i$ values evaluated at the same σ_a value. This is due perhaps to the effects of damage to the structure due to shear deformation (Flora et al., 1994).

For analysis, the following relationship was assumed based on the laboratory test results shown above;

$$E^e=(E^e)_0\cdot(\sigma_v/\sigma_0)^m \tag{13}$$

where E^e is the current undamaged elastic Young's modulus in the vertical direction obtained at a vertical stress σ_v, $(E^e)_0$ is the value of E^e when σ_v is equal to a certain value σ_0 and m is the power and is equal to 0.57.

The tangent modulus E_{tan}, defined for total axial strain increments (i.e., plastic plus elastic axial strain increments) during primary loading, decreases with the increase in the stress ratio q/q_{max} where q_{max} is the compressive strength. Since the increase in the axial stress contributes to the increase in E_{tan} through the increase in E^e, the relationship between the ratio E_{tan}/E^e and q/q_{max} may be more appropriate for modeling the non-linear deformation characteristics during shearing. Figure 10 shows a plot of data obtained from the triaxial compression tests at σ_c=0.2, 0.5 and 0.8 kgf/cm^2 (19.6, 49 and 78.4 kPa). It can be seen that the relationships are essentially independent of σ_3. The average of these relationships together with Eq. (13) will be used to estimate the compression of a geosynthetic-reinforced gravel mass subjected to vertical load.

For a preloaded/prestressed (PL/PS) geosynthetic-reinforced soil retaining wall (GRS-RW) shown in Fig. 11, the compression of the gravel mass upon the application of vertical load $(P_C)_{max}$=120 tonf (1.18 MN) at the top block is computed below. It is noted that P_C=120 tonf is

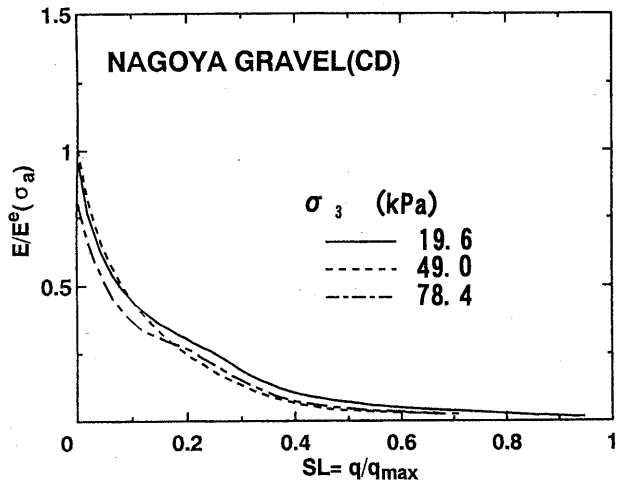

Fig. 10. Relationship between the ratio of the tangent Young's moduli E_{tan} to E^e (Eq. (13)) and the stress ratio q/q_{max} for a well compacted well-graded gravel used as a backfill material of the GRS bridge abutments in Nagoya (reproduction from Dong et al., 1994)

equivalent to half the deadload of a reinforced concrete bridge girder for a single railway track having a length as long as 20–30 m. This is much longer than the present longest length of a bridge girder of 13.2 m supported by a GRS retaining wall (Tatsuoka and Tateyama, 1995). The gravel type considered herein is that used at the GRS-RWs at Nagoya (Figs. 8–10). The area of the block is 1.5 m × 4 m (i.e., A = 6 m^2), the wall height H is 5 m, the total unit weight γ of the gravel is 2.25 gf/cm^3 (2.21 kN/m^3), $(E^e)_0$ = 4,000 kgf/cm^2 (392 MPa) for σ_0 = 1.0 kgf/m^2 (98 kPa), m = 0.57, the initial vertical load P_0 due to the weight of the top block is 7.2 tonf (70.6 kN); A(=6 m^2) × thickness(=0.5 m) × the unit weight of reinforced concrete (2.4 tonf/m^3 or 2.35 kN/m^3), and the total stiffness of the four rods K_{rod} = 3.3 × 10^5 kgf/cm (3.2 × 10^5 kN/m). It is assumed that the gravel mass with a cross-sectional area equal to A is subjected to the same average stress increment P_C/A throughout the wall height. The effects of the rigid facing are ignored.

The current elastic Young's modulus E_{eq} at a depth z from the top of the gravel mass is assumed to be equal to E^e (Eq. (13)) and obtained as:

$$E_{eq}=(E^e)_0\cdot\{(\sigma_{s0}+\gamma\cdot z)/\sigma_0\}^m \tag{14}$$

where σ_{s0} is the vertical stress σ_s at z = 0. When the vertical load P_C is applied as primary load (i.e., the case without both preloading and prestressing) and increased

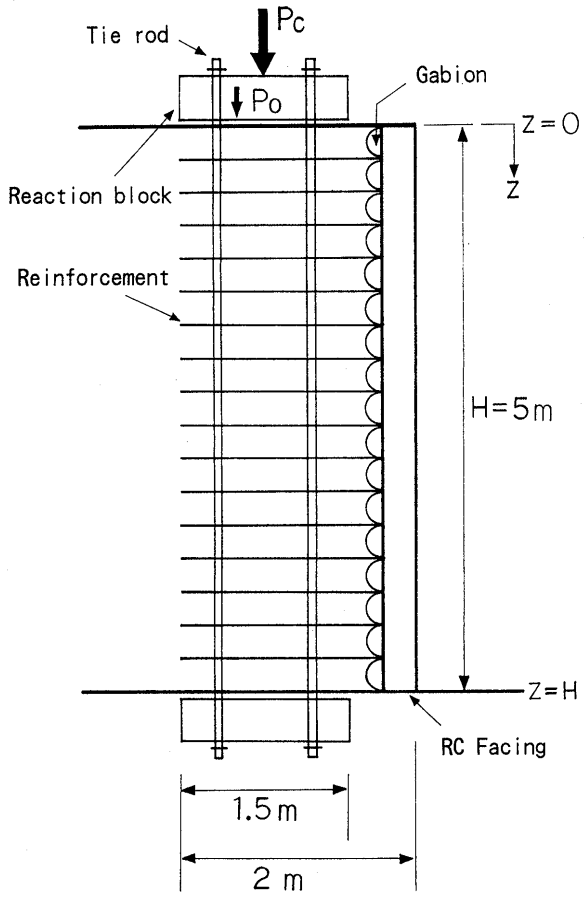

Fig. 11. A model preloaded/prestressed geosynthetic-reinforced gravel retaining wall

to the maximum value $(P_C)_{max}$, the settlement S_1 of the top block caused by the application of $(P_C)_{max}$ on the top block is obtained as:

$$S_1=\int_0^H \varepsilon_s(z)\cdot dz \tag{15}$$

where $\varepsilon_s(z)$ is the strain in the gravel at the depth z due to load $(P_C)_{max}$, which is obtained as:

$$\varepsilon_s(z)=\int_{(\sigma_s)_i}^{(\sigma_s)_p} d\sigma_s/E_{tan} \tag{16}$$

where σ_s is the current vertical stress at z obtained as;

$$\sigma_s=\sigma_{s0}+\gamma\cdot z,\quad \sigma_{s0}=\frac{P_0+P_C}{A} \tag{17}$$

$(\sigma_s)_i$ and $(\sigma_s)_p$ are the initial and peak values of σ_s given by;

$$(\sigma_s)_i=\frac{P_0}{A}+\gamma\cdot z,\quad (\sigma_s)_p=\frac{P_0+(P_C)_{max}}{A}+\gamma\cdot z \tag{18}$$

E_{tan} is the current tangent Young's modulus for primary loading given by;

$$E_{tan}=R\cdot E^e\quad (R=0.195) \tag{19}$$

where R is equal to E_{tan}/E^e, which is a function of the shear stress level q/q_{max} (Fig. 10). In this approximate calculation, the value of q/q_{max} is assumed to be constant, equal to 0.3, throughout loading to $(P_C)_{max}$. This is equivalent to assuming a constant earth-pressure coefficient. The E^e value is obtained from Eq. (13). S_1 = 1.05 cm is then obtained.

Next, the case where the procedure for preloading and prestressing with a certain preload value P_{PL} and the rod tension T_P as prestress equal to 60 tonf (588 kN) is considered. The settlement S_2 of the top block caused by the application of $(P_C)_{max}$ is then obtained as;

$$S_2=\int_0^H \varepsilon_s(z)\cdot dz \tag{20}$$

$\varepsilon_s(z)$ is obtained by assuming $E_{eq}=E^e$ (Eq. (14)) as;

$$\varepsilon_s(z)=\int_{(\sigma_s)_i}^{(\sigma_s)_p} d\sigma_s/E^e \tag{21}$$

where

$$(\sigma_s)_i=\frac{P_0+T_P}{A}+\gamma\cdot z \tag{22}$$

The value of $(\sigma_s)_p$ is the peak value of σ_s resulting from the application of $(P_C)_{max}$ = 120 tonf (1.18 MN), which is obtained numerically as shown below. The value of E_{eq} is obtained from Eq. (14). The force equilibrium, corresponding to Eq. (7), is;

before the application of P_C

$$P_0=(\sigma_{s0})_i\cdot A-T_P \tag{23a}$$

after the application of P_C

$$P_0+P_C=\sigma_{s0}\cdot A-T \tag{23b}$$

where T is the total tensile force in the four tie rods induced by the application of P_C. The tensile strain increment $\Delta\varepsilon_t$ in the tie rods due to the application of P_C, which is negative, is obtained from;

$$T_P - T = K_{rod} \cdot (-\Delta\varepsilon_t) \cdot H \tag{24}$$

Since the compression of the tie rods between the top and bottom blocks, which is equal to $\Delta\varepsilon_t \cdot H$, should be equal to the compression of the gravel mass S_2, we obtain from Eqs. (15) and (24);

$$T = T_P - K_{rod} \int_0^H \varepsilon_s(z) \cdot dz \tag{25}$$

By substituting Eq. (25) into Eq. (23b), we obtain;

$$\sigma_{s0} = \frac{P_0 + T_P + P_C}{A} - \frac{K_{rod}}{A} \int_0^H \varepsilon_s(z) \cdot dz \tag{26}$$

Since $\varepsilon_s(z)$ is a function of P_C, the relationship between the average contact pressure σ_{s0} and P_C is obtained by numerical integration (Fig. 12). The curves below and above point a show the relationships when the force in the tie rods is in tension and zero, respectively. In this case, $(\sigma_{s0})_p = 25.2$ tonf/m^2 (247 kPa) is obtained. The increase in the contact pressure σ_{s0} by the application of $(P_C)_{max}$ is equal to $2.52 \times p_a - 1.12 \times p_a = 1.4 \times p_a$ (p_a=98 kPa), which is smaller than $(P_C)_{max}/A = 2.0 \times p_a$ when

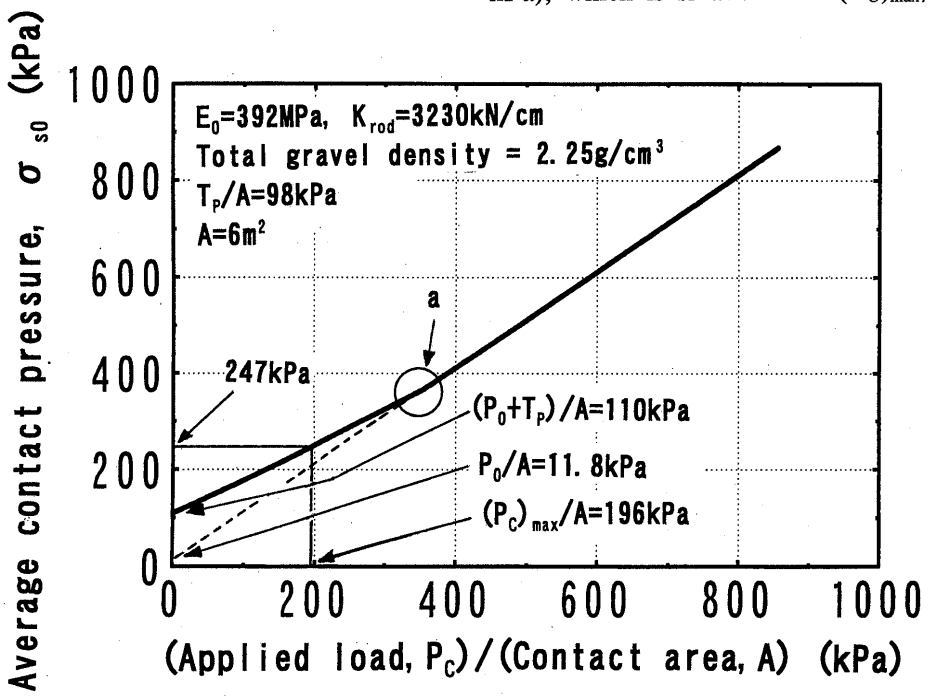

Fig. 12. Relationship between the average vertical pressure σ_{s0} at the top of the gravel mass and the vertical load P_C for the reinforced wall model shown in Fig. 11

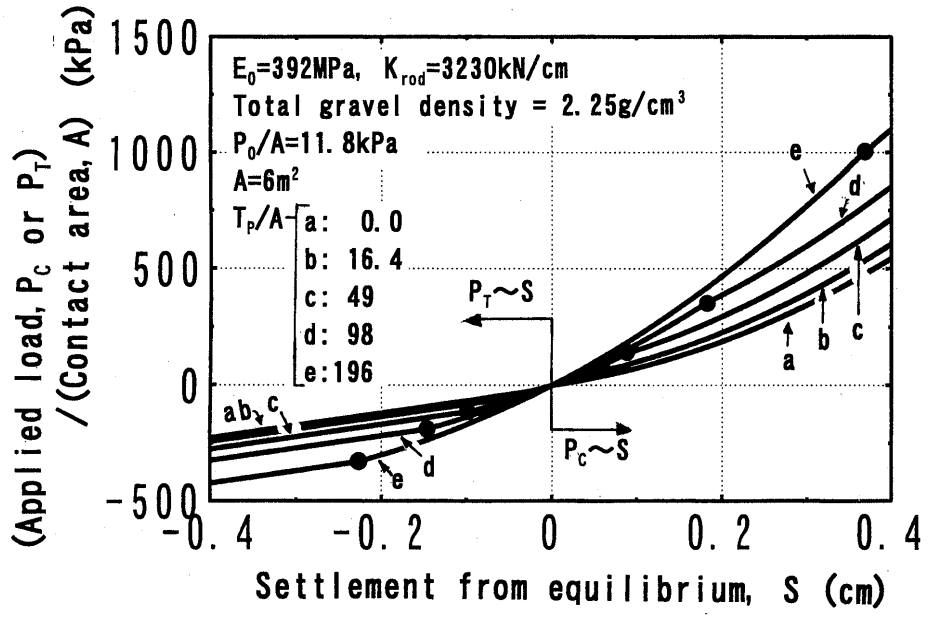

Fig. 13. Effects of preloading and prestressing calculated following the methods shown in this paper (infinitively large P_{PL} is assumed)

prestress T_P is equal to zero. The value $(\sigma_{s0})_p = \{P_0 + T_P + (P_C)_{max}\}/A$ equal to $3.12 \times p_a$ is attained when K_{rod} is negligible as compared with K_{soil} (n.b., this case is discussed later).

The stress value $\sigma_s(z) = \sigma_{s0} + \gamma \cdot z$ for a given value of P_C is obtained from Eq. (26), which results in a value of $E_{eq} = E^e$ (Eq. (14)), and then the value of $\varepsilon_s(z)$ (Eq. (21)), and finally, S_2 (Eq. (20)) are obtained. The value of S_2 thus calculated is 0.11 cm, which is much smaller than the value of S_1 (=1.05 cm). The difference is due to the combined effects of preloading and prestressing. The average vertical strain in the gravel mass with S_2 is as small as $S_2/H = 0.022\%$, which indicates that the gravel mass would behave nearly elastically upon the application of $(P_C)_{max} = 120$ tonf (1.18 MN). This small strain is in accordance with the assumption used (i.e., elastic behaviour of the gravel). In this case, the remaining value of T upon the application of $(P_C)_{max}$ is obtained as;

$$T = T_P - K_{rod} \cdot (-\Delta\varepsilon_t) \cdot H = T_P - K_{rod} \cdot S_2$$
$$= 60 \text{ tonf}(588 \text{ kN}) - 36.3 \text{ tonf}(356 \text{ kN})$$
$$= 23.7 \text{ tonf}(232 \text{ kN}) \quad (27)$$

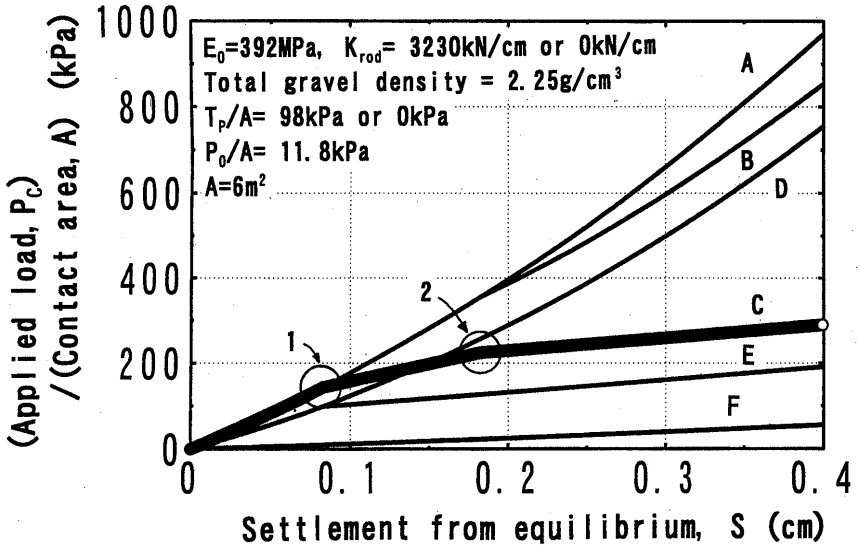

Case	K_{rod}	P_{PL}	T_P
A (2)	3230 kN/cm (3.3×10⁵ kgf/cm)	Very large (1)	0.59 MN (60 tonf)
B (3)			
C		1.18 MN (120tonf)	
D	0 kN/cm	Very large (1)	
E		1.18 MN (120tonf)	
F	Not considered.	0 MN	0 MN

1) P_{PL} is large enough so that only elastic soil strains will occur within the limit of P_C considered here.
2) It is assumed that the tie rods exhibit the same rigidity when in compression as when in tension.
3) $K_{rod} = 0$ when the tie rods are in compression.

Fig. 14. Effects of preloading and prestressing together with those of K_{rod} in the case of compressive external load (calculated as those shown in Fig. 13)

Figure 13 shows the relationships between the vertical load (P_C or P_T) and the vertical displacement of the top block occurring from the equilibrium state. To observe the effects of prestress first, the relationships are obtained when the preload P_{PL} is infinitively large, while the prestress T_P is changed from zero to 120 tonf (1.8 MN). The other data remains the same. The relationship for each of the compressive and tensile vertical loads has a "kink" when the tension in the tie rods disappears (i.e., the transition is not smooth) or when the top reaction block loses the contact with the gravel surface. The external load at the moment when the tensile force in the tie rods disappears depends on K_{soil}, K_{rod}, the preload value P_{PL} and the prestress value T_P. Larger prestress tension T_P should be introduced in advance so that tension can exist in the tie rods upon the application of external load. At the same time, it should be confirmed that the preload value P_{PL} is large enough so that the gravel exhibits essentially elasticity when the compressive external load is applied. It would be a reasonable practice to employ a preload value P_{PL} that exceeds $(P_C)_{max}+T_P$.

Figure 14 shows the effects of preloading and prestressing for the case of compressive external load. In this figure, the relationships for tie rod rigidity of $K_{rod}=0$ are also shown (i.e., the cases D and E; this will be discussed later). Cases A~E assume the same prestress $T_P=60$ tonf (0.59 MN). Case A shows the upper-bound rigidity when P_{PL} is infinite and it is assumed that the tie rods can exhibit the same rigidity when in compression as when in tension (n.b., this assumption is not realistic). Case B assumes the same P_{PL} as case A, but it is assumed that the tie rods in compression has no rigidity. Case C is the most realistic one. The first change in slope, denoted by the number 1, indicates the beginning of the plastic deformation of soil, while the second change, the number 2, shows that the tension in the tie rods vanishes. For the occurrence of plastic deformation, the tangential Young's modulus E_{tan} obtained from Fig. 10 is used. Case F shows the behaviour when no preload and prestress is employed. It can be readily seen from Fig. 13 that the effects of preloading and prestressing are significant. Since this calculation is based on several assumptions, these results should be investigated by appropriate full-scale tests.

FEASIBILITY OF THE PROPOSED METHOD

One of the important aspects of this proposed method is how long sufficiently large prestress can survive without significant stress relaxation. In order to evaluate this point and others, full-scale test walls were constructed in the beginning of 1995 at the Chiba Experiment Station, Institute of Industrial Science, University of Tokyo (Fig. 15). The test facility has four test sections, separated by reinforced concrete (RC) walls having a thickness of 60 cm that have been firmly anchored into the subsoil profile. The distance between the adjacent RC walls is fixed by connecting the top ends with a number of steel stiffeners after the model soil wall segments were constructed. Sections Nos. 1, 2 and 4 are geosynthetic-reinforced retaining walls with a backfill of volcanic ash clay (Kanto loam). Section 4 has a cantilever RC retaining wall with an unreinforced clay backfill (test segment 4N) and is not discussed in this paper. Section 3 has three test segments of grid-reinforced gravel (Fig. 16(a) and (b),

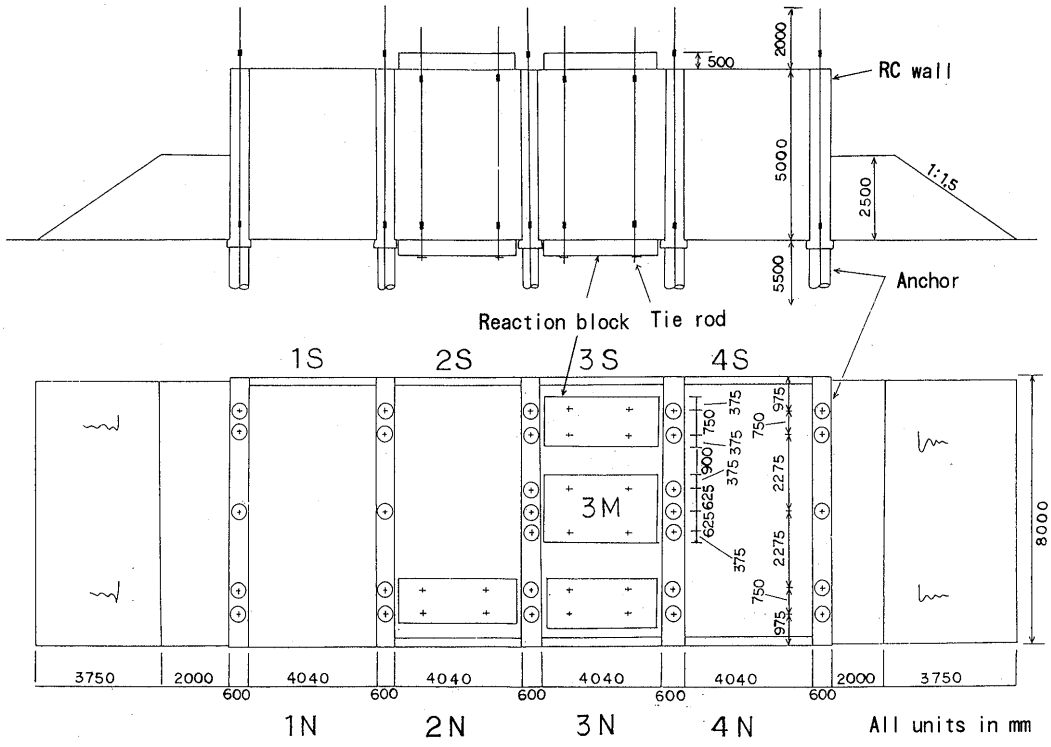

Fig. 15. a) Longitudinal vertical cross-section, b) Plan of full-scale test walls constructed at Chiba Experiment Station, IIS, University of Tokyo

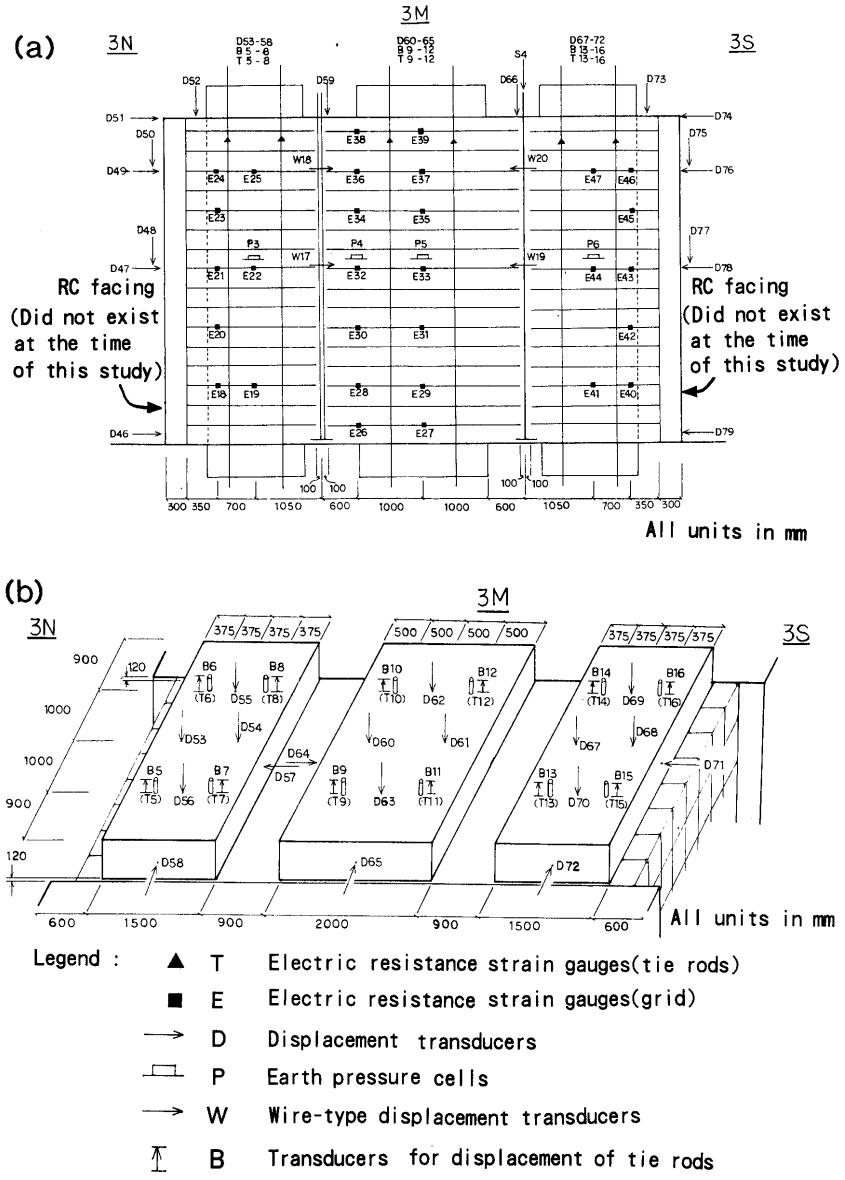

Fig. 16. Cross-section and crest of the section 3 having three test segments of grid-reinforced gravel

Photo. 1). The south and north walls (test segment 3S and 3N) have the same basic configuration as the one shown in Fig. 11 (i.e., have a wrapped-around wall face constructed with a help of gabions filled with gravel, Photo. 2). The central test segment 3M is separated from 3S and 3N by an unreinforced gravel zone with a thickness of 0.2 m. A full height RC facing will be constructed on each of the wall faces after the present study into the effects of preloading and prestressing has been completed.

A well-graded gravel of crushed sandstone, which was used to obtain the data shown in Fig. 5, was compacted to a total density γ_t of about 2.01 tonf/m^3 with an average water content of 7.0%. The field density was measured using the water-replacement method. The density was not as high as expected, perhaps because only a small compaction machine could be used due to the space limitation (Photo. 3). In actual construction projects for

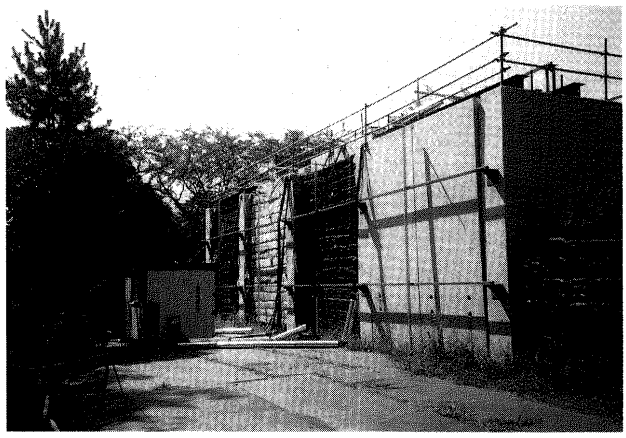

Photo. 1. View of the walls (from the right, the walls 4N, 3N, 2N and 1N)

GRS retaining walls (RWs), a much larger compaction machine is used (*see* Photo. 1, page 340, Tatsuoka et al., 1994a). The grid is made of PVA (polyvinyl alcohol with the trade mark 'Vinylon') having a nominal tensile rupture strength of 7.5 tonf/m (73.5 kN/m). This type of grid has been used to construct GRS-RWs as railway structures for a total length of more than 20 km. Photograph 4 shows a view of the bottom of test segments 3S, 3M and 3N, where three base RC blocks having a thickness of 0.5 m, with four tie rods protected with a PVC tube extending from each block, have been constructed. Photograph 5 shows a view of the top of test segments 3S, 3M and 3N.

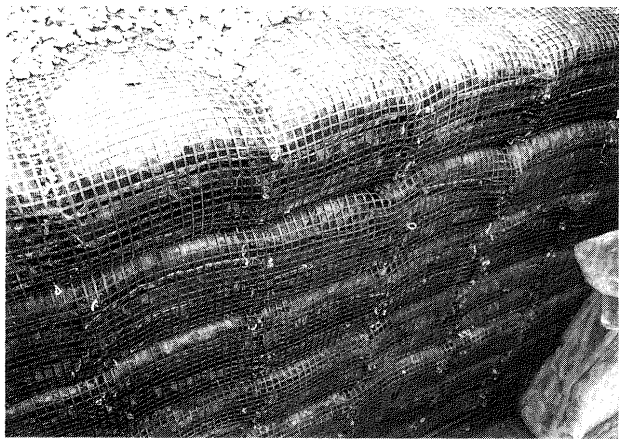

Photo. 2. Wrapped-around wall face of wall segment 3N

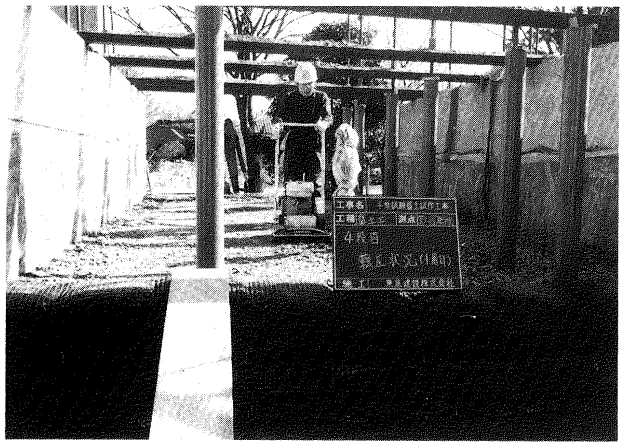

Photo. 3. Compaction using a small compaction machine

Photo. 4. A view of the bottom of test segments 3S to 3N

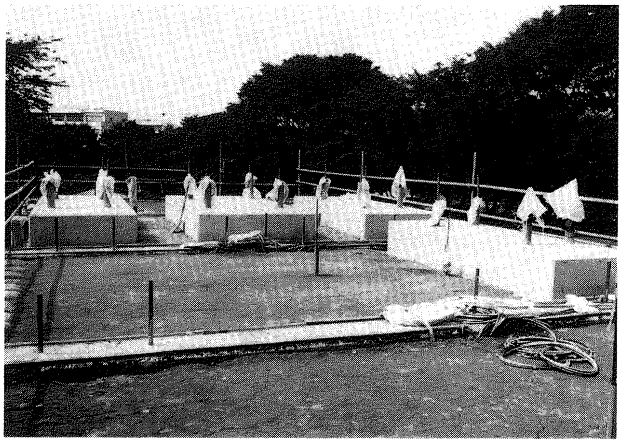

Photo. 5. A view of the top of test segments 3S to 3N

The walls were completed at the end of April 1995, followed by the construction of the top RC blocks in the middle of May 1995. At the end of August 1995, preloading of test segments 3S, 3N and 3M was started by using four center-hole hydraulic jacks (Fig. 17). As seen from

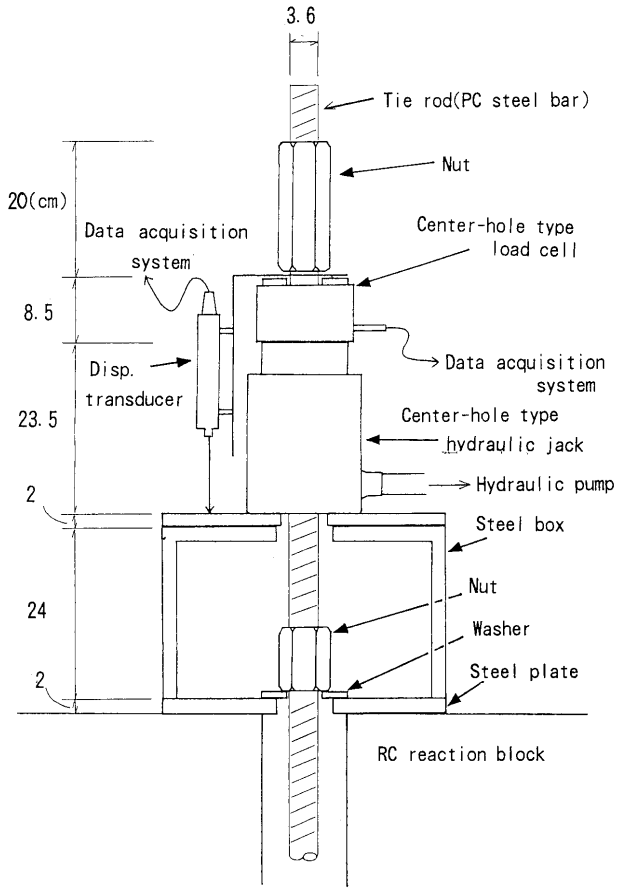

Fig. 17. Details of the jacking system for each tie rod placed on the top reaction block

Fig. 18(a), for segment 3S, the first preload which was equal to 704 kN {12.6 tonf/m^2 (123 kPa) times A (=5.7 m^2)} was introduced and was maintained for only about ten minutes. It was confirmed from the measurements of strain in reinforcements and earth pressure that the backfill soil was loaded similarly throughout the wall height. The top ends of the four rods were then fixed to the top block, while releasing the pressure in the hydraulic jacks. The tensile force in the tie rods dropped suddenly by about one fourth of the preload, probably due to the inevitable slack between the nut-washer system at the top end of each tie rod and the top RC block (Fig. 17). This decrease in the tensile force seemed to be repetitive and happened to be nearly equivalent to the planned amount of unloading. The relaxation in the tie rod tension with time was then monitored.

The test procedure for segment 3N was similar (Fig. 18(b)), except that creep deformation was allowed to occur for 63 hours under the preloading condition, during which the top block settled about 1.3 cm.

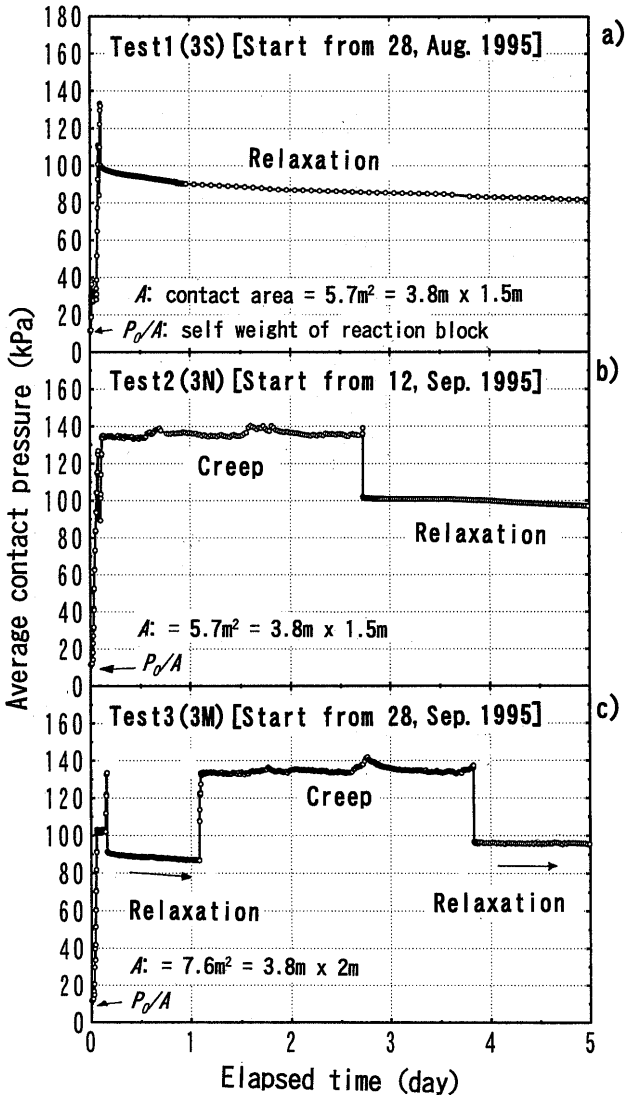

Fig. 18. Time histories of the average contact pressure $(P_0+T_P)/A$ at the top RC block from the end of August 1995; a) 3S, b) 3N and c) 3M

Segment 3M has a top RC block with a larger cross-sectional area that is equal to 2 m × 3.8 m = 7.6 m^2. Nearly the same average pressure was applied during preloading (Fig. 18(c)). The stress relaxation was allowed to occur for 72 hours after a very small amount of creep deformation that occurred only for two hours at an average contact pressure equal to 1.05 kgf/cm^2 (103 kPa), which was lower than the prescribed preload. After a relatively large rate of stress relaxation was observed, the preload was applied again and maintained for 66 hours. The creep settlement was about 0.7 cm, which is much smaller than that observed for segment 3N under nearly the same preloading period. The difference would be due to the fact that the RC block for segment 3M is larger and the gravel at segment 3M was better compacted since it was located at the center of the crest of the fill.

The summary of the time histories of the average contact pressure plotted against time is shown in Fig. 19. Figure 20 shows the relationship between the average pressure P_C/A and the average settlement of the top RC block in segment 3M.

The following trends of behavior may be noted from

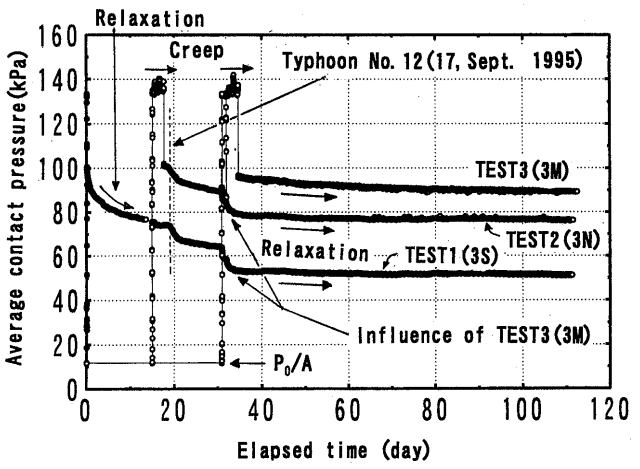

Fig. 19. Summary of the time histories of the average contact pressure $(P_0+T_P)/A$ at the top RC block from the end of August 1995, 3S, 3N and 3M

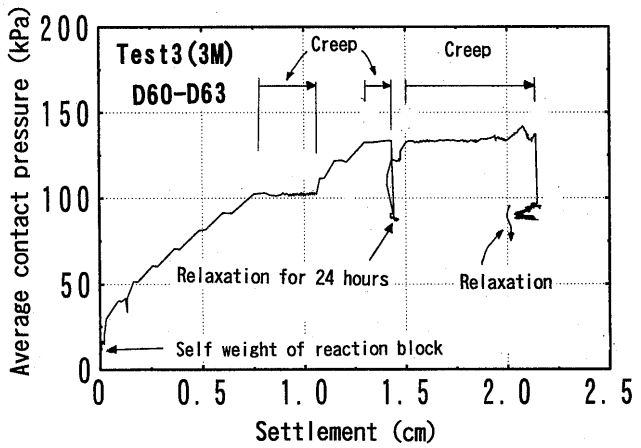

Fig. 20. Relationship between the average contact pressure $(P_0+T_P)/A$ and the average settlement of the top RC block, segment 3M

Figs. 18, 19 and 20:

1) When a noticeable amount of creep deformation was not allowed to occur during preloading (segment 3S and the first preloading for segment 3M), the rate of stress relaxation immediately after unloading was very high.

2) By having allowed some noticeable amount of creep deformation to occur during preloading (segment 3N and the second preloading for segment 3M), the rate of stress relaxation was very low. This was particularly the case with the second relaxation for segment 3M when compared with the first relaxation.

3) A sudden increase in relaxation rate was observed on 17th September 1995. This was due to heavy rain with a total precipitation of more than 130 mm resulting from Typhoon No. 12, which passed the site. Since the gravel had an initial water content of about 7.0% with a fines content of 8.0%, it seems that a degree of suction was created during compaction, part of which may have been lost by moisting the material. If the wall deformed due to the backfill soil becoming wet, then it should have been very small, since displacement transducers did not detect any noticeable wall deformation. This factor will have to be studied in the future.

4) When preload was applied to segment 3M, a noticeable reduction was observed in the tie rod tension in segments 3N and 3S, which would be likely due to the associated compression of the gravel in these segments.

5) The relaxation rate in segment 3M after the second unloading and segments 3S and 3N after preloading segment 3M was very low. It is notable that the reduction in the tie rod tension in segments 3S and 3N was practically zero for a duration of the last two months. In addition, the average reduction rate in segment 3M was only about 0.013 tonf/m^2/day (0.13 kPa/day) for the last one month, and this value decreased with time.

6) The vertical stiffness of the wall was much larger when reloaded than when primarily loaded (Fig. 20). This is due mostly to the effect of preloading.

The results indicate a high feasibility of the application of this construction method to actual construction projects. The details of the full-scale model tests will be reported by the authors elsewhere.

The results of the field model tests described above have not been analyzed by the model explained in the preceding section, simply because sufficient deformation and strength properties of the backfill material (i.e., gravel) has not been evaluated by triaxial compression tests. Such analysis will be performed in later.

DISCUSSION

A well-graded gravel of crushed sandstone was used for this model walls, considering that when this type of gravel is well compacted, it can have a high stiffness value and may have a very low creep deformation rate. In addition, this type of gravel has been used as the backfill soil for GRS bridge abutments (e.g., Fig. 7). The use of another type of soil for this construction method is being attempted by the authors; i.e., the backfill soil of test segment 2S is a clay (volcanic ash clay, Kanto loam), in which preloading and prestressing has been applied. It was found that viscous effects are more pronounced in the clay backfill. It was also found that similar to the case of the gravel backfill, the creep and relaxation rate decreases substantially by allowing a sufficient amount of creep deformation to occur during the preloading stage. Some of the results for the clay backfill are reported by Tatsuoka et al. (1996).

From a practical point of view, it is first required that the instantaneous settlement at the top of the wall upon the application of large dead weight, such as a bridge girder or a building structure, would be small. It is also required that the long-term creep deformation which may result is also small.

To achieve small instantaneous settlements, the rigidity K_{soil} of soil during reloading should be large enough. This behaviour can be seen in Fig. 20. Secondly, the sufficiently large prestress should exist for a long duration. Based on the results shown in Figs. 18 and 19, it seems that it is quite feasible to sustain sufficiently high prestress. When the time schedule of construction can be controlled, it may be possible to re-introduce prestress in advance. In order to determine whether or not sufficiently high prestress can survive for a long duration so as to be effective for live load at later stages, the effects of traffic load, heavy rainfall, seismic load and seasonal temperature variations on the tie rod tension should be evaluated by further study.

As the tie rod rigidity K_{rod} increases, the rate of the creep deformation of a prestressed soil mass for a given external load (i.e., the rate of the settlement of the top block) becomes smaller, while the rate of stress relaxation becomes larger (Fig. 21). The block settles with time at a slope of $1/K_{rod}$ of the relationship between the axial load on the top of the soil $\sigma_{s0} \cdot A$ and the block settlement S from a given time denoted as a at time $t=0$. Therefore,

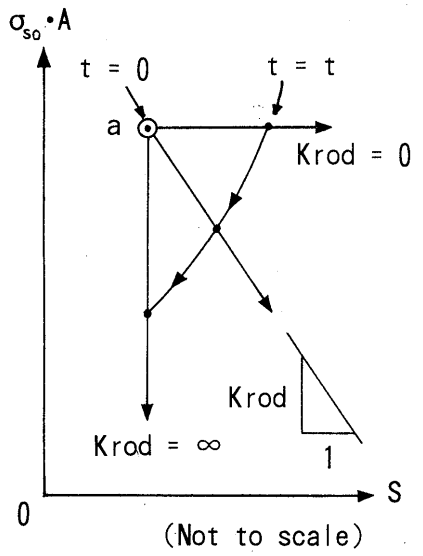

Fig. 21. Effects of the tie rod rigidity K_{rod} on the rate of creep deformation and the rate of stress relaxation for a given constant external load

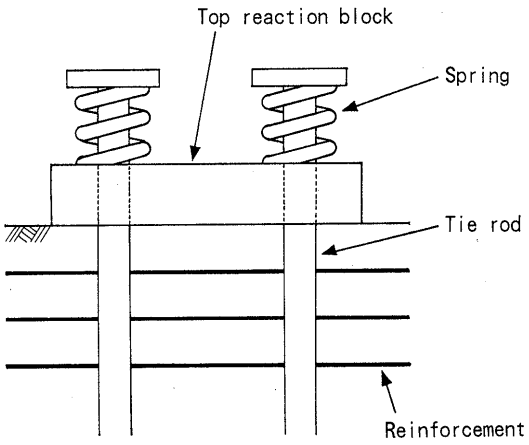

Fig. 22. Prestressing with a spring at the top of each tie rod

when K_{rod} is practically negligible, the block settles at a constant soil pressure without any stress relaxation. When K_{rod} is infinitively large, the compressive stress in the soil and the tensile stress in the tie rods relax with time without settlement of the block.

To preserve as large as possible a prestress, the use of a spring system at the top of each rod after preloading (Fig. 22) would be effective. The tie rod rigidity K_{rod} then becomes very low. In this case, when an external load P_C is applied, the load increment will be supported mostly by the soil mass, but the tensile force in the tie rods will decrease only slightly, contributing only in a small way to decreasing the settlement. That is, the settlement S_2 (Eq. (20)) is obtained by using a very small value of K_{rod}. The prestress, however, will be maintained and contribute to decreasing the settlement by maintaining a high vertical confining pressure. This point can be seen from Fig. 14 by comparing the curves for Cases D and E with $K_{rod}=0$ with those for the large K_{rod} value. The yield value of P_C/A for Case E is controlled by the preload P_{PL}/A. This method may be useful when the rate of stress relaxation is too large due to a large K_{rod} value while re-prestressing is not feasible. If feasible, therefore, the best method would be the use of such a system where the K_{rod} value is very small after preloading, while it can be made very large immediately before $(P_C)_{max}$ is applied.

It may be concluded that the appropriate K_{rod} value to be selected, therefore, depends on many factors including the feasibility of re-prestressing and the requirements for instantaneous and long-term settlements at the top block level.

POSSIBLE APPLICATIONS

Several conceivable applications of the proposed construction method to actual construction projects may be the following:

1) GRS bridge abutments (Fig. 7): In this application, prestress will contribute also to reducing the outward shear deformation of the wall caused by the outward lateral load (e.g., seismic loads) through an increase in the soil shear stiffness. For the same reason, cyclic shear strains during earthquake will be reduced, which will result in the reduction of dynamic compaction of a backfill soil due to seismic force.

2) Preloading and prestressing the backfill soil behind a bridge abutment: Using this method, the problem of long-term residual settlement of the backfill relative to a bridge abutment supported by a pile foundation may be solved practically.

3) Geosynthetic-reinforced soil to support a structure (Fig. 23): This method will substantially reduce the settlement of the fill upon the construction of a heavy structure, thus making a pile foundation unnecessary. This method will also be effective to reduce the possible rock-

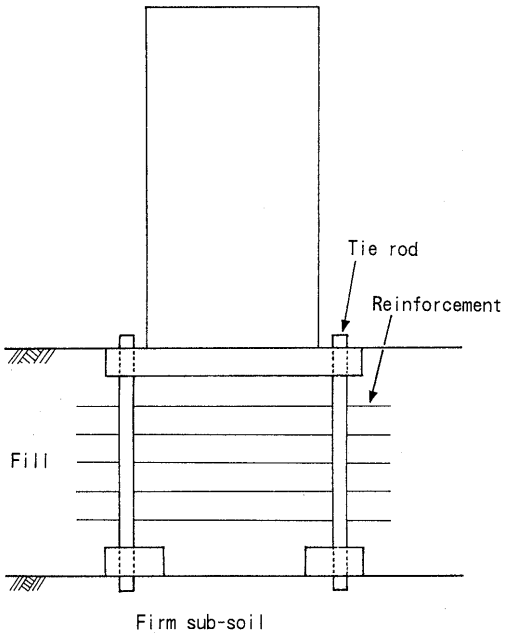

Fig. 23. One of the possible applications for a fill supporting a heavy structure

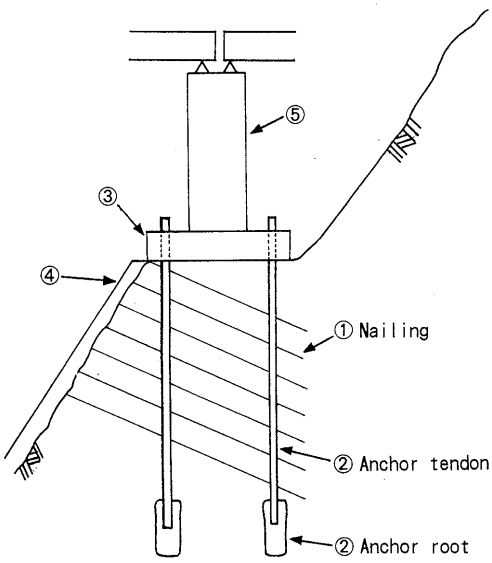

Fig. 24. One of possible applications for a slope supporting a tall heavy structure

ing motion of the structure during earthquake (Luong, 1990, 1991).

4) Nailed soil slope supporting a heavy tall structure (Fig. 24): The principle of PL/PS can also be applied to a slope excavated with soil nailing (① in Fig. 24). Several vertical anchors ② are installed from the foundation area on the slope crest. PL/PS is then introduced with the help of RC block ③ on the crest. When required, a facing ④ is constructed on the slope face before the main structure ⑤ is constructed. In this case, when the slope is under nearly plane strain conditions, the deformation of the slope when preloaded could be effectively restrained. Some measures should otherwise be taken, for example, nailing in the directions inclined in the horizontal plane.

CONCLUSIONS

A new and unique construction method was proposed, which can substantially reduce the settlement experienced by a heavy structure that is constructed on a reinforced soil mass. In this method, the advantages of the effects of preloading and prestressing on the stiffness of soil are utilized. The mechanism in this structure can be summarized as;

1) a large reduction of plastic deformation of soil by preloading,
2) high stiffness of soil from prestressing,
3) high stiffness of an integrated structure consisting of a soil mass and tie rods by prestressing, and
4) prestressing of lateral reinforcement members by preloading.

The working example and the result of a full-scale test indicate that the application of this new construction method to actual construction projects is quite feasible at least when the backfill is a well-compacted well-graded gravel. A couple of the issues to be studied in the future are addressed, and finally several feasible applications are suggested.

ACKNOWLEDGEMENTS

The authors are deeply indebted to their colleagues for their help in performing this study, particularly, Dr. J. Koseki, Dr. T. Kodaka, Mr. T. Sato, Dr. G.-L. Jiang, Mr. K. Muramoto, Mr. R. Motohiro, and Mr. H. Shibata, Valuable suggestions were given by Prof. H. Di Benedetto, DGCB, ENTPE, France, and the valuable review comments by Prof. Dov Leshchinsky and Dr. H.-I. Ling, University of Delaware, USA, are gratefully acknowledged.

REFERENCES

1) Di Benedetto, H. (1983): "Modélisation du comportement des geomateriaux: application aux enrobes bitumineux et aux bitumes," Thése de D.E., ENTP-USTMG-INPG.
2) Di Benedetto, H. and Tatsuoka, F. (1996): "Small strain behaviour of geomaterials: modelling of the strain rate effects," Soils and Foundations, Vol. 37, No. 2, pp. 127-138.
3) Dong, J., Nakamura, K., Tatsuoka, F. and Kohata, Y. (1994): "Deformation characteristics of gravels in triaxial compression tests and cyclic triaxial tests," Int. Symp. on Pre-Failure Deformation Characteristics of Geomaterials, Shibuya et al. (eds.), IS Hokkaido '94, Vol. 1, pp. 17-23.
4) Flora, A., Jiang, G. L., Kohata, Y. and Tatsuoka, F. (1994): "Small strain behaviour of a gravel along some triaxial stress paths," Proc. of Int. Symp. on Pre-Failure Deformation Characteristics of Geomaterials, Shibuya et al. (eds.), IS Hokkaido '94, Vol. 1, pp. 279-285.
5) Goto, S., Tatsuoka, F., Shibuya, S., Kim, Y.-S. and Sato, T. (1991): "A simple gauge for local small strain measurements in the laboratory," Soils and Foundations, Vol. 31, No. 1, pp. 169-180.
6) Hoque, E., Tatsuoka, F., Sato, T. and Kohata, Y. (1995): Inherent and stress-induced anisotropy in small-strain stiffness of granular materials," Proc. 1st Int. Conf. of Earthquake Geotechnical Engineering, IS Tokyo '95, Ishihara (ed.), Vol. 1, pp. 277-282.
7) Huang, C.-C. and Tatsuoka, F. (1990): "Bearing capacity of reinforced horizontal sandy ground," Geotextiles and Geomembranes, Vol. 9, pp. 51-82.
8) Jiang, G.-L. (1996): "Deformation characteristics of dense well-graded gravels evaluated by triaxial tests," Dr. Eng. Thesis, University of Tokyo.
9) Kohata, Y., Tatsuoka, F., Dong, J., Teachavorasinskun, S. and Mizumoto, K. (1994): "Stress states affecting elastic deformation moduli of geomaterials," Proc. of Int. Symp. on Pre-Failure Deformation Characteristics of Geomaterials, Shibuya et al. (eds.), IS Hokkaido '94, Vol. 1, pp. 3-9.
10) Luong, M. P. (1990): "Prestressed foundations for slender structures subject to dynamic loadings," Earthquake Resistant Construction and Design, Savidis (ed.), Balkema, pp. 503-513.
11) Luong, M. P. (1991): "Modeling prestressed foundation for overhead line structures," Centrifuge 91, Ko (ed.), Balkema, pp. 217-224.
12) McGown, A., Yeo, K. C. and Yogarajah, I. (1991): "Identification of a dynamic interlock mechanism," Performance of Reinforced Soil Structures, McGown (eds.), British Geotechnical Society, Thomas Telford, pp. 377-379.
13) Tatsuoka, F., Murata, O. and Tateyama, M. (1992): "Permanent geosynthetic-reinforced soil retaining walls used for railway embankment in Japan," Geosynthetic-Reinforced Retaining Walls, Wu (ed.), Balkema, pp. 101-130.
14) Tatsuoka, F., Tateyama, M., Murata, O. and Tamura, Y. (1994a): Closure to the discussion by Mr. Pierre Segrestin, Recent Case Histories of Permanent Geosynthetic-Reinforced Soil Retaining Walls, Tatsuoka and Leshchinsky (eds.), Balkema, pp. 323-342.
15) Tatsuoka, F., Sato, T., Park, C. S., Kim, Y. S., Mukabi, J. N. and Kohata,Y. (1994b): "Measurements of elastic properties of geomaterials in laboratory compression tests," Geotec. Testing J., ASTM, Vol. 17, No. 1, pp. 80-94.
16) Tatsuoka, F., "Teachavorasinskun,S., Dong, J., Kohata, Y. and Sato, T. (1995): Importance of measuring local strains in cyclic triaxial tests on granular materials," Dynamic Geotechnical Testing: Second Volume, ASTM STP 1213, Edelhar, Drnevich and Kutter (eds.), pp. 288-302.
17) Tatsuoka, F. and Kohata, Y. (1995): "Stiffness of hard soils and soft rocks in engineering applications," Keynote Lecture, Int. Symp. on Pre-Failure Deformation Characteristics of Geomaterials, Shibuya et al. (eds.), IS Hokkaido '94, Vol. 2, pp. 947-1063.
18) Tatsuoka, F. and Tateyama, M. (1995): "Geotextile-reinforced soil retaining walls," Kiso-ko (the Foundation Engineering and Equipment), Vol. 29, No. 23, pp. 84-92 (in Japanese).
19) Tatsuoka, F., Uchimura, T., Tateyama, M. and Muramoto, K. (1996): "Creep deformation and stress relaxation in preloaded/prestressed geosynthetic-reinforced soil retaining walls," Proc. ASCE '96 "Measuring and Modeling Time-Dependent Soil Behavior", ASCE Washington Convention, pp. 228-278.